Complexation ability of tetrasulfosubstituted cobalt(II) phthalocyanine toward ORF3a protein of SARS-CoV-2 virus

O. I. Koifman,[a,b]* V. E. Maizlish,[b] M. O. Koifman,[a,b] N. Sh. Lebedeva,[a] E. S. Yurina,[a] Yu. A. Gubarev,[a]* and E. L. Gur'ev[c]

[a]G. A. Krestov Institute of Solution Chemistry, Russian Academy of Sciences,
1 ul. Akademicheskaya, 153045 Ivanovo, Russian Federation.
E-mail: gua@isc-ras.ru
[b]Ivanovo State University of Chemistry and Technology,
7 Sheremetevskii prosp., 153000 Ivanovo, Russian Federation
[c]Lobachesky State University of Nizhny Novgorod,
4 Ashkhabadskaya ul., 603105 Nizhny Novgorod, Russian Federation

Complex formation processes of tetrasulfosubstituted cobalt(II) phthalocyanine with ORF3a accessory protein of SARS-CoV-2 coronavirus were studied. The interaction of ORF3a protein with SARS-CoV-2 virus with tetrasulfosubstituted cobalt(II) phthalocyanine affords a stable complex in which metallophthalocyanine exists in the monomeric form. The complex formation induces slight changes in the secondary structure of the protein by increasing the fraction of disordered fragments of the polypeptide chain. The photoirradiation of the complex of ORF3a protein of SARS-CoV-2 virus with tetrasulfosubstituted cobalt(II) phthalocyanine leads to the photooxidation of amino acid residues of the protein.

Key words: phthalocyanine, protein, virus SARS-CoV-2, complex formation, photooxidation.

Severe acute respiratory syndrome coronavirus (SARS-CoV-2) is the pathogen of COVID-19. Virion SARS-CoV-2 contains a single-chain RNA and 28 specific proteins grouped into 16 non-structured proteins (from Nsp1 to Nsp16), four basic proteins (spike (S), membrane (M), nucleocapsid (N), envelope protein (E)), and eight accessory proteins (ORF3a, ORF6, ORF7a, ORF7b, ORF8, ORF9b, ORF9c, and ORF10).[2—5] Each of them perform its function and participates in diverse stages of the viral infection.[6] Specific features of their binding with various ligands are being actively studied presently.[7,8] It is reliably known that accessory proteins are not involved in virus replication but play the decisive role in host—virus interactions and in the modulation of immune response of the host, which induces cytokine storm.[9—11] One of the most important proteins for pathogenesis of COVID-19 is the ORF3a protein, which is the largest (275 amino acids) accessory and unique membrane protein. Protein ORF3a is responsible for virulence, infectivity, activity of ionic channels, and morphogenesis and release of virus. An analysis of the recombinant virus with ORF3a deficient shows that ORF3a is insufficient for SARS-CoV-2 replication *in vitro* and *in vivo* but makes a determining contribution to viral pathogenesis.[12] Expression of ORF3a induces the activation of NF-κB (NF-kappaB is the transcription factor controlling gene expression of immune response, apoptosis, and cell cycle) and induces chemokine generation, fragmentation of Golgi's apparatus, endoplasmic reticulum stress, accumulation of intracellular bubbles, and cell decay.[13—15] The ORF3a protein is a viroporin, and the activity of this protein as a ionic channel is necessary because of its pro-apoptotic properties. The ORF3a interacts with caveolin and suppresses the transmission of IFN

---

* Oscar Iosifovich Koifman, born in 1944, Doctor of Chemical Sciences, Professor, President of the Ivanovo State University of Chemistry and Technology (Ivanovo, Russia), leading scientist in the field of macroheterocyclic tetrapyrrole compounds, honored worker of science of the Russian Federation, awarded by prizes of the President of RF and Government of RF and the Order of Honor, elected the Full Member (Academician) of the Russian Academy of Sciences in 2022 (for more detailed information, see Ref. 1).

signals of type I, but enhances fibrinogen secretion, which favors cytokine storm.[16] Therefore, the ORF3a protein can become an important therapeutic target. Hence, it seems significant to find compounds forming a strong complex with this protein, since this interaction can provide the inhibition of the main protein functions and, probably, would allow one to correct an immune response of the organism to viral infection and would lead to an adequate functioning of autophagy and apoptosis mechanisms.

Macroheterocyclic compounds (MHCs) possess a unique set of physicochemical properties, and the insertion of peripheral substituents of various nature can provide a solubility in water of the indicated compounds and can also increase their selectivity and strength of binding with these or other protein fragments.[17−21] Another important property of MHCs is their ability to generate (upon photoirradiation) singlet oxygen both in the individual state and in complexes with proteins.[22] The generation of singlet oxygen by MHCs in complexes with proteins can result in irreversible changes in both the secondary and primary protein structure, which would finally provide a viricidal action of MHCs. Compounds corresponding to the listed above conditions, particularly, cobalt(II) tetrasulfosubstituted phthalocyanine (CoPc), were isolated in the previous work[23] devoted to the molecular modeling of ORF3a protein coupling with a number of MHCs. Therefore, the purpose of the present study was the study of complex formation processes of the ORF3a protein with CoPc and evaluation of protein damage upon the photoirradiation of the complexes.

CoPc
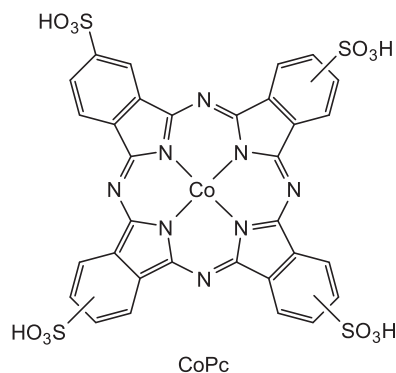
Results and Discussion

The electronic absorption spectrum (EAS) of cobalt(II) tetrasulfophthalocyanine in a phosphate buffer is shown in Fig. 1.
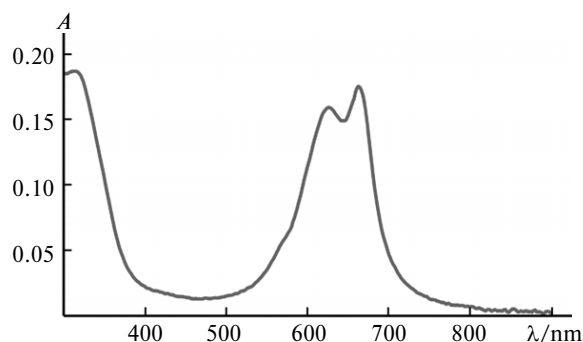

Fig. 1. Electronic absorption spectrum of cobalt(II) tetrasulfophthalocyanine ($1.1 \cdot 10^{-5}$ mol L^{-1}) in a phosphate buffer.

According to the obtained EAS, tetrasulfosubstituted cobalt(II) phthalocyanine exists in a phosphate-buffered saline (PBS, pH 7.4) in the partially dimerized state in spite of relatively high solubility in water caused by four peripheral sulfo groups. The absorption of the dimeric forms of MHCs is detected in a range of 629 nm, and the absorption maximum of the monomeric forms of MHCs is observed at 665 nm. A probable reason for the equilibrium

$$2\,CoPc \rightleftharpoons (CoPc)_2 \qquad (1)$$

is a high concentration of electrolytes in the PBS with pH 7.4, which provides osmomolarity of the buffer solution equal to the blood osmomolarity. The total amount of anions and cations in the PBS results in a decrease in the amount of free water for the hydration of CoPc. In addition, a high concentration of electrolytes in the PBS favors a partial neutralization of negative charges of sulfo groups of CoPc and a decrease in the electrostatic repulsion between the adjacent likely charged fragments of CoPc, which results in their self-association.

The EAS of ORF3a in the PBS are shown in Fig. 2.

The absorption in a range of 200—300 nm is typical of proteins. The EAS of the ORF3a protein exhibits two absorption maxima at 200—230 and 278 nm, and the absorption bands are asymmetric. It is known that the absorption bands of the peptide bonds are located in a range of 190—220 nm, and the absorption maxima of aromatic amino acids are detected in the near-UV range (275—282 nm). The ORF3a composition includes 45 aromatic amino acids: 14 phenylalanine, 17 tyrosine, eight histidine, and six tryptophan residues with the absorption maxima at the wavelengths 257, 272, 270, and 280 nm, respectively. We believe that the high light scattering can be due to ORF3a dimers, since the
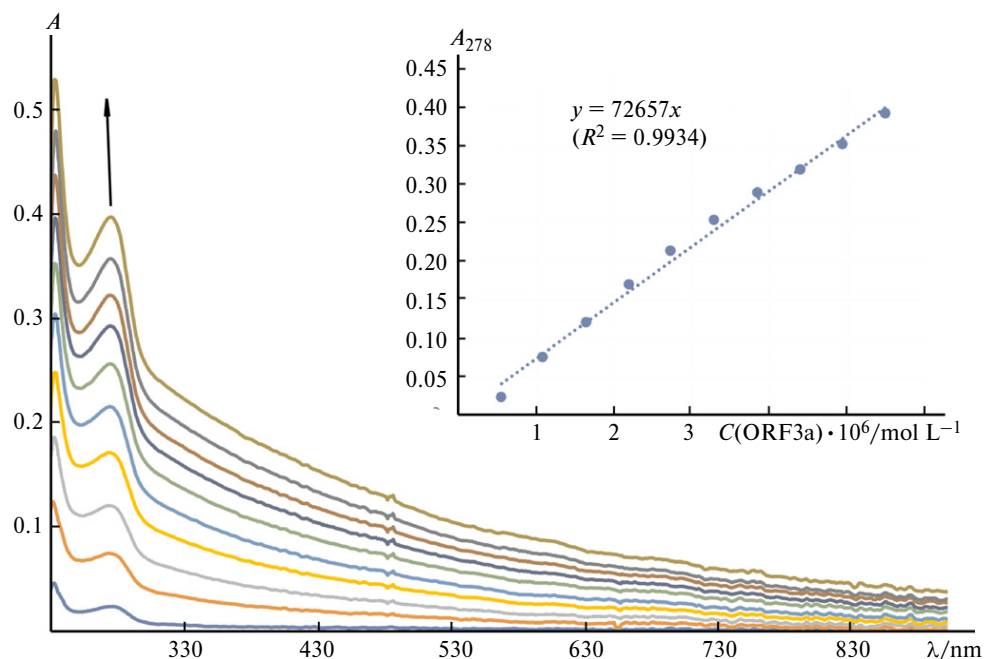
Fig. 2. Electronic absorption spectra of ORF3a ($5.5 \cdot 10^{-7}$—$5.5 \cdot 10^{-6}$ mol L^{-1}) in PBS; inset: absorbance at $\lambda = 278$ nm (A_{278}) *vs* concentration of ORF3a in PBS; arrow shows the direction of increasing ORF3a concentration.

most part of the ORF3a protein of coronaviruses is known to function *in vivo* in the dimeric form.[15,24] The electrophoresis results show that a portion of the protein exists in the dimeric form in the studied solutions, since the bands at the molecular weights about 63 and 70 kDa are detected according to the markers. The consecutive increase in the protein concentration (see Fig. 2) results in an increase in the absorbance of the solutions, and the character of the change is linear (see Fig. 2, inset). This indicates that no changes occur in self-aggregation when the protein concentration is varied from $5.5 \cdot 10^{-7}$ to $5.5 \cdot 10^{-6}$ mol L^{-1}.

The results of spectrophotometric titration of a solution of CoPc ($1.1 \cdot 10^{-5}$ mol L^{-1}) with a solution of the ORF3a protein (Fig. 3) will be considered below.

A decrease in the intensity in the absorption ranges of both the MHC dimer and monomer is observed at the initial stage of titration. A further increase in the protein concentration, a change in the CoPc : ORF3a molar ratio from 7 : 1 to 2 : 1, results in a decrease in the absorption intensity at 625 nm (absorption of the dimer) and an increase in the absorption intensity of the monomer. These spectral changes unambiguously characterize the shift of equilibrium (1) toward monomerization. In addition,

a phenomenon unusual for metallophthalocyanines was observed: bathochromic shift of the absorption Q band upon complex formation, which is 12 nm in the system under study. The shift of the Q band indicates that the solvate/pseudo-solvate environment of CoPc has changed: probably, CoPc becomes surrounded by amino acid residues of the protein upon complex formation. According to the molecular docking results,[23] CoPc is predominantly bound in the immediate vicinity to domain V of the ORF3a
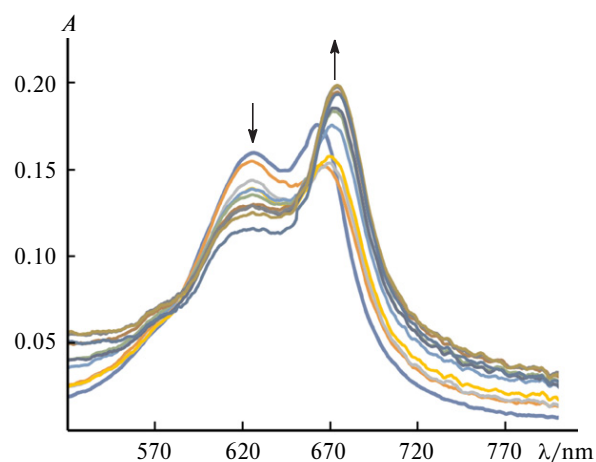

Fig. 3. Electronic absorption spectra of CoPc during titration with ORF3a in PBS.

protein (amino acid residues 160—163).[25] This is a conservative motif inherent in the whole line of coronaviruses and involved in the transport of the ORF3a protein from Golgi´s apparatus to cellular and intracellular membranes, lipid droplets, and lysosomes. Domain V is responsible for the intracellular transport of ORF3a. According to the molecular docking results, the CoPc complex with the ORF3a protein is stabilized due to the formation of several hydrogen bonds between the oxygen atoms of the peripheral SO_3^- groups and amino acid residues Lys66a, Lys67a, Arg68a, Tyr141a, Asp183a, Glu181a, Asp210b, Lys235b, Asp210a, Lys235a, Lys67b, Arg68b, Tyr141b, and Asp183b, where a and b are the ORF3a proteins in the dimer. Unfortunately, the performed IR spectral study did not allow us to confirm or reject hydrogen bond formation involving the SO_3^- groups of CoPc. This is caused by the fact that the characteristic frequencies of SO_3^- vibrations arranged in the ranges 1350—1250 and 1100—1000 cm^{-1} are not identified in the spectrum of the complex with the protein, which is spectrally active in this spectral range. The secondary structure of the ORF3a protein changes after binding with CoPc: an inversion of the absorption intensity at 1638 and 1617 cm^{-1} is observed in the Amide I range, and in the Amide III range the vibration band at 1254 cm^{-1}

shifts to the high-frequency range by 6 cm^{-1}. This indicates an increase in the fraction of disordered fragments of the polypeptide chain upon CoPc binding.

The synthesized 1 : 1 complex of the ORF3a protein with CoPc was photoirradiated with the visible light (400—700 nm) for 1 h. The obtained sample was studied by IR spectroscopy and using the western blot method. The IR spectrum of the irradiated protein complex with CoPc differs substantially from the initial sample (Fig. 4). As can be seen from the recorded IR spectra, the photoirradiation results in substantial changes in the spectrum: new bands appear, a number of bands disappears, and the ratio of intensities of the most part of bands changes. All the data described indicates a change in both the secondary and primary structures of the protein. The study by the electrophoresis method revealed a smear in the range below 20 kDa (Fig. 5).

Thus, the complex formation processes of the ORF3a protein of the SARS-CoV-2 virus with tetrasulfosubstituted cobalt(II) phthalocyanine were studied for the first time. The formation of the complex was proved using spectral methods. The binding of CoPc by the protein was found to exert an insignificant effect on the secondary protein structure by increasing the fraction of disordered fragments. The
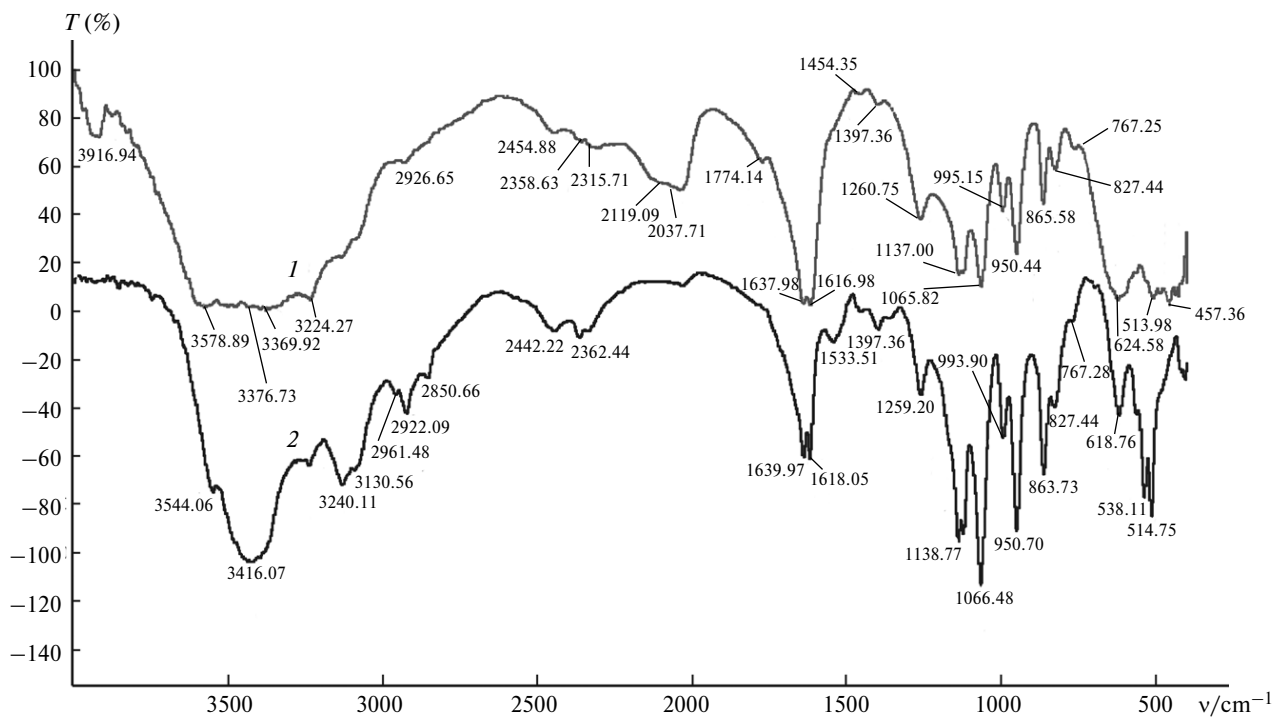

Fig. 4. IR spectra of the initial (*1*) and irradiated (*2*) complex of ORF3a with CoPc in KBr.
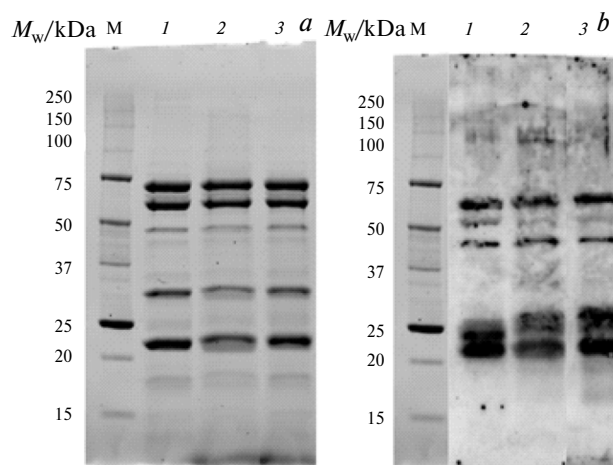
Fig. 5. Results of electrophoresis (*a*) and immunoblotting (*b*) of ORF3a protein before and after incubation with CoPc; M are markers of the molecular weight; *1*, initial ORF3a protein; *2*, complex of ORF3a with CoPc; and *3*, irradiated complex of ORF3a with CoPc.

photoirradiation of the protein complex with CoPc results in changes in both the secondary and primary structures of the protein. The results obtained demonstrate that CoPc can be a potential active drug capable of changing the primary protein structure upon photoirradiation.

Experimental

Electronic absorption spectra were recorded on an AvaSpec-2048 spectrometer (Avantes GmbH, Holland) in quartz tubes with an optical path length of 10 mm at 25 °C in a temperature-maintained cell. IR spectra were detected on an Avatar 360 FT-IR spectrometer (Thermo Nicolet, USA) in a range of 4000—500 cm^{-1} in KBr pellets. ^{1}H NMR spectra were obtained on a Bruker Avance-500 instrument (USA) using tetramethylsilane as the internal standard. MALDI-TOF mass spectra of positive ions were measured on a Shimandzu AXIMA Confidence time-of-flight mass spectrometer with matrix-associated laser desorption (Japan) and on a Bruker Daltonics Ultraflex instrument (USA). Elemental analysis was carried out on a FlashEA 1112 analyzer (Thermo Electron Corp., Italy).

The ORF3a protein was expressed at the Lobachesky State University of Nizhny Novgorod in two stages. Plasmids pGBW-m4046959 (AddGene #145722) bearing target protein sequences were used as the matrix for the polymerase chain reaction (PCR). Authenticity of the obtained protein samples was determined by immunoblotting with antibodies to the oligohistidine sequence localized on the C-end of the proteins.

The solution was irradiated with a white photodiode lamp (400—700 nm) with a power of 10 W in plastic conic 200-µL microtubes at 25 °C for 1 h. The light was directed to the tubes from above, and the distance from the lamp to the tubes was 5 cm.

Cobalt(II) tetrasulfophthalocyanine was synthesized and purified according to earlier described procedures.[26] The degree of purity of the used tetrasulfophthalocyanine was at least 98%. EAS (DMSO), λ_{max} (logε): 664 (5.15), 602 (4.50), 330 (4.85). ^{1}H NMR (D$_2$O), δ: 10.02 (br.s), 9.76 (br.s), 8.68 (br.s), 8.38 (br.s), 8.09 (m), 7.87 (m). MS MALDI-TOF MS: found m/z 891.53 [M]$^+$; calculated for C$_{32}$H$_{16}$CoN$_8$O$_{12}$S$_4$ 891.71. Found (%): C, 42.62; H, 1.89; N, 12.38; O, 22.01; S, 14.11. C$_{32}$H$_{16}$CoN$_8$O$_8$S$_4$. Calculated (%): C, 43.10; H, 1.81; N, 12.57; O, 21.53; S, 14.38.

Spectrophotometric studies were carried out in a solution of phosphate-buffered saline (PBS) (Merck) at pH 7.4.

No human or animal subjects were used in this research.

The authors declare no competing interests.

References

1. Election of the Full Members (Academicians), Corresponding Members, and Foreign Members of the Russian Academy of Sciences, *Russ. Chem. Bull.*, 2022, **71**, 1559; DOI: 10.1007/s11172-022-3565-4.
2. J. Díaz, *Front. Physiol.*, 2020, **11**, 870; DOI: 10.3389/fphys.2020.00870.
3. F. J. Barrantes, *Acta Crystallogr. D*, 2021, **77**, 391; DOI: 10.1107/S2059798321001431.
4. X. Li, E. E. Giorgi, M. H. Marichannegowda, B. Foley, C. Xiao, X.-P. Kong, Y. Chen, S. Gnanakaran, B. Korber, F. Gao, *Sci. Adv.*, 2020, **6**, No. 27, eabb9153; DOI: 10.1126/sciadv.abb9153.
5. A. Yu, A. J. Pak, P. He, V. Monje-Galvan, L. Casalino, Z. Gaieb, A. C. Dommer, R. E. Amaro, G. A. Voth, *Biophys. J.*, 2021, **120**, 1097; DOI: 10.1016/j.bpj.2020.10.048.
6. F. N. Novikov, V. S. Stroylov, I. V. Svitanko, V. E. Nebolsin, *Russ. Chem. Rev.*, 2020, **89**, 858; DOI: 10.1070/RCR4961.
7. V. S. Stroylov, I. V. Svitanko, *Mendeleev Commun.*, 2020, **30**, 419; DOI: g/10.1016/j.mencom.2020.07.004.
8. C. Zhang, C. Zhang, Y. Meng, T. Li, Z. Jin, S. Hou, C. Hu, *Mendeleev Commun.*, 2022, **32**, 334; DOI: 10.1016/j.mencom.2022.05.013.
9. Y. Ren, T. Shu, D. Wu, J. Mu, C. Wang, M. Huang, Y. Han, X.-Y. Zhang, W. Zhou, Y. Qiu, *Celluar Mol. Immun.*, 2020, **17**, 881; DOI: 10.1038/s41423-020-0485-9.

10. V. Marquez-Miranda, M. Rojas, Y. Duarte, I. Diaz-Franulic, M. Holmgren, R. E. Cachau, F. D. Gonzalez-Nilo, *bioRxiv*, 2020; DOI: 10.1101/2020.10.22.349522.

11. Y.-J. Tan, P.-Y. Tham, D. Z. Chan, C.-F. Chou, S. Shen, B. C. Fielding, T. H. Tan, S. G. Lim, W. Hong, *J. Virol.*, 2005, **79**, 10083; DOI: 10.1128/JVI.79.15.10083-10087.2005.

12. B. Yount, R. S. Roberts, A. C. Sims, D. Deming, M. B. Frieman, J. Sparks, M. R. Denison, N. Davis, R. S. Baric, *J. Virol.*, 2005, **79**, 14909; DOI: 10.1128/JVI.79.23.14909-14922.2005.

13. K. Narayanan, C. Huang, S. Makino, *Virus Res.*, 2008, **133**, No. 1, 113—121; DOI: 10.1016/j.virusres.2007.10.009.

14. J. Steward, *Drug Target Review*, 2020.

15. R. Minakshi, K. Padhan, M. Rani, N. Khan, F. Ahmad, S. Jameel, *PloS one*, 2009, **4**, No. 12, e8342; DOI: 10.1371/journal.pone.0008342.

16. D. M. Kern, B. Sorum, S. S. Mali, C. M. Hoel, S. Sridharan, J. P. Remis, D. B. Toso, A. Kotecha, D. M. Bautista, S. G. Brohawn, *Nat. Struct. Mol. Biol.*, 2021, **28**, 573; DOI: 10.1038/s41594-021-00642-1.

17. O. I. Koifman, T. A. Ageeva, I. P. Beletskaya, A. D. Averin, A. A. Yakushev, L. G. Tomilova, E. S. Yurina, *Macroheterocycles*, 2020, No. 13, 311; DOI: 10.6060/mhc200814k.

18. N. F. Goldshleger, M. A. Lapshina, V. E. Baulin, A. A. Shiryaev, Yu. G. Gorbunova, A. Yu. Tcivadze, *Russ. Chem. Bull.*, 2020, **69**, 1223; DOI: 10.1007/s11172-020-2893-5.

19. A. A. Botnar, N. P. Domareva, K. Yu. Kazarian, T. V. Tikhomirova, M. B. Abramova, A. S. Vashurin, *Russ. Chem. Bull.*, 2022, **71**, 953; DOI: 10.1007/s11172-022-3496-0.

20. N. G. Bichan, E. N. Ovchenkova, *Russ. Chem. Bull.*, 2021, **70**, 239; DOI: 10.1007/s11172-021-3081-y.

21. A. S. Malyasova, E. A. Kostrova, I. G. Abramov, V. E. Maizlish, O. I. Koifman, *Russ. Chem. Bull.*, 2021, **70**, 2405; DOI: 10.1007/s11172-021-3360-7.

22. V. F. Otvagin, N. S. Kuzmina, L. V. Krylova, A. B. Volovetsky, A. V. Nyuchev, I. V. Balalaeva, A. Y. Fedorov, A. E. Gavryushin, I. N. Meshkov, Y. G. Gorbunova, Y. V. Romanenko, O. I. Koifman, *J. Med. Chem.*, 2019, **62**, 11182; DOI: 10.1021/acs.jmedchem.9b01294.

23. N. S. Lebedeva, Y. A. Gubarev, G. M. Mamardashvili, S. V. Zaitceva, S. A. Zdanovich, A. S. Malyasova, J. V. Romanenko, M. O. Koifman, O. I. Koifman, *Sci. Rep.*, 2021, **11**, No.1, 1—12; DOI: 10.1038/s41598-021-99072-8.

24. Y. Yue, N. R. Nabar, C.-S. Shi, O. Kamenyeva, X. Xiao, I.-Y. Hwang, M. Wang, J. H. Kehrl, *Cell Death Dis*, 2018, **9**, 904; DOI: 10.1038/s41419-018-0917-y.

25. E. Issa, G. Merhi, B. Panossian, T. Salloum, S. Tokajian, *Msystems*, 2020, **5**, No. 3, e00266-00220; DOI: 10.1128/mSystems.00266-20.

26. G. Shaposhnikov, V. Kulinich, V. Maizlish, *Modifitsirovannye ftalotsianiny i ikh strukturnye analogi* [*Modified Phthalocyanines and Their Structural Analogs*], Krasand, Moscow, 2012, 480 pp. (in Russian).